AEM
Journals.ASM.org

Transcriptomic Responses of *Phanerochaete chrysosporium* to Oak Acetonic Extracts: Focus on a New Glutathione Transferase

Anne Thuillier,[a,b] Kamel Chibani,[a,b] Gemma Belli,[c] Enrique Herrero,[c] Stéphane Dumarçay,[d] Philippe Gérardin,[d] Annegret Kohler,[a,b] Aurélie Deroy,[a,b] Tiphaine Dhalleine,[a,b] Raphael Bchini,[a,b] Jean-Pierre Jacquot,[a,b] Eric Gelhaye,[a,b] Mélanie Morel-Rouhier[a,b]

Université de Lorraine, IAM, UMR 1136, IFR 110 EFABA, Champenoux, France[a]; INRA, IAM, UMR 1136, Vandoeuvre-les-Nancy, France[b]; Departament de Ciències Mèdiques Bàsiques, Universitat de Lleida, IRB Lleida, Lleida, Spain[c]; Université de Lorraine, LERMAB, UMR 1093, Faculté des Sciences et Technologies, Vandoeuvre-lès-Nancy, France[d]

The first steps of wood degradation by fungi lead to the release of toxic compounds known as extractives. To better understand how lignolytic fungi cope with the toxicity of these molecules, a transcriptomic analysis of *Phanerochaete chrysosporium* genes was performed in the presence of oak acetonic extracts. It reveals that in complement to the extracellular machinery of degradation, intracellular antioxidant and detoxification systems contribute to the lignolytic capabilities of fungi, presumably by preventing cellular damages and maintaining fungal health. Focusing on these systems, a glutathione transferase (*P. chrysosporium* GTT2.1 [PcGTT2.1]) has been selected for functional characterization. This enzyme, not characterized so far in basidiomycetes, has been classified first as a GTT2 compared to the *Saccharomyces cerevisiae* isoform. However, a deeper analysis shows that the GTT2.1 isoform has evolved functionally to reduce lipid peroxidation by recognizing high-molecular-weight peroxides as substrates. Moreover, the GTT2.1 gene has been lost in some non-wood-decay fungi. This example suggests that the intracellular detoxification system evolved concomitantly with the extracellular ligninolytic machinery in relation to the capacity of fungi to degrade wood.

Lignolytic basidiomycetes initiate wood decay by producing extracellular reactive oxygen species (ROS) that depolymerize lignocellulose (1, 2). Accordingly, induction of lignin peroxidases (LiPs) is associated with ROS production, oxidative damage to macromolecules, and induction of antioxidant enzymes, such as catalase, superoxide dismutase (SOD), glutathione (GSH) reductase (GR), and glutathione peroxidase (Gpx) (3). In wood-grown *Postia placenta*, the quantity of ROS produced by a laccase has been estimated to be large enough to contribute to incipient decay (2). Moreover, some highly reactive wood compounds (known as extractives) are released primarily during wood degradation processes. Some studies have reported the toxicity and antifungal activity of these molecules (4–7). This suggests that during wood degradation, fungal cells are under oxidative stress.

Thus, the lignolytic activity of fungi is closely related to their capacity to resist oxidants and toxic molecules, such as wood extractives or fungicides. Thus, fungi have developed an efficient detoxification system. It is composed of enzymes encoded by multigenic families, which are expanded in these genomes and exhibit versatile activities, allowing them to accept a broad range of compounds such as substrates (8, 9). This system is composed mainly of oxidases as cytochrome P450 monooxygenases (CytP450), conjugating enzymes, and transporters. CytP450-encoding genes are highly represented in saprophytic fungal genomes (10–12). Functional analysis and gene upregulation data suggested that the enriched P450 families of model basidiomycetes have a common physiological function, i.e., degradation of plant defense chemicals and plant material-derived compounds, especially lignin-derived compounds (13). Moreover, the catalytic versatility of these enzymes could be involved in fungal colonization of plant material. CytP450 copy numbers in the genomes of wood degraders is correlated with the glutathione transferase (GST) copy numbers (11). GST genes belong to the second step of detoxification and participate in cell response to oxidative stress. They are less duplicated than CytP450s, but saprotrophic fungi, such as the wood decayer *Phanerochaete chrysosporium* or the litter decomposer *Coprinus cinereus*, still exhibit a high number of GST-encoding genes compared to symbiotic fungi or biotrophic pathogens (11). *P. chrysosporium* exhibits 27 GST isoforms, which cluster into 7 main classes: GSTO, GHR, Ure2p, GSTFuA, GTT1, GTT2, and Phi (11). The cysteine-containing GSTs (GSTO and GHR) are quite well conserved among organisms and have been studied in humans, insects, plants, and fungi (11). The others are more specific to some organisms and have been studied less. In particular, GSTFuA, which has been described recently, is a fungus-specific class with atypical features (14). Some GSTFuA members exhibit a ligandin property with wood-related molecules. GTT1 and GTT2 are described exclusively in *Saccharomyces cerevisiae*, having an antioxidant role (15). While *S. cerevisiae* GTT2 (ScGTT2) displays only classical GST activity, ScGTT1 exhibits both classical GST activity and peroxidase activity with hydroperoxides (16). The crystal structure of ScGTT2 has been solved (17). A water molecule acts as the deprotonator of the glutathione sulfur atom instead of the classic catalytic residues, i.e., tyrosine, serine, and cysteine. To date, no other fungal homologue has been characterized. In *P. chrysosporium*, 2 GTT2-related (Joint Genome Institute [JGI] protein identifiers [ProtID] 6683 and 6766) and no GTT1

Received 26 June 2014 **Accepted** 1 August 2014
Published ahead of print 8 August 2014
Editor: D. Cullen
Address correspondence to Mélanie Morel-Rouhier, Melanie.Morel@univ-lorraine.fr.
Supplemental material for this article may be found at http://dx.doi.org/10.1128/AEM.02103-14.

doi:10.1128/AEM.02103-14

genes have been identified in the genome by sequence homology with the yeast isoforms (18). However, their roles are unknown.

The aim of this study was to better understand how *P. chrysosporium* copes with the putative toxicity of oak acetonic extracts. Using a transcriptomic approach, we show that oak acetonic extracts create oxidative stress in *P. chrysosporium* highlighted by induction of genes of the antioxidant and detoxification systems. In particular, the analysis has revealed the induction of the gene coding for *P. chrysosporium* GTT2.1 (PcGTT2.1), a GTT2-related glutathione transferase, which is highly active against peroxides and seems to have evolved concomitantly with the extracellular degradation system.

MATERIALS AND METHODS

Oak acetonic extract preparation and identification. Oak heartwood samples were ground to a fine powder, passed through a 115-mesh sieve, and dried at 60°C until minimal weight was obtained. Extraction then was performed overnight with high-performance liquid chromatography (HPLC)-grade acetone using a Soxhlet apparatus. The solvent was removed from the crude extracts by evaporation to dryness under vacuum. The powder was resuspended in dimethyl sulfoxide (DMSO). Liquid chromatography-mass spectrometry (LC-MS) analyses of samples were carried out using a Shimadzu (Noisiel, France) LC-20A ultra-HPLC (UHPLC) system equipped with an autosampler and interfaced to a PDA UV detector SPD-20A, followed by an LC-MS 8030 triple-quadruple mass spectrometer. The separation was performed on a Luna C_{18} analytical column (inner diameter, 150 mm by 3 mm; Phenomenex, Le Pecq, France) using a linear gradient from 8 to 68% of methanol in water (containing 0.1% formic acid) at a flow rate of 0.4 ml/min. The injection volume was 2 μl. UV-visible spectra were recorded between 190 and 800 nm. Positive and negative ion electrospray mass spectrometric analyses were carried out at a unit resolution between 100 and 2,000 *m/z* at a scan speed of 15,000 U/s. The heat block and desolvation line temperatures were 400°C and 250°C, respectively. Nitrogen was used as a drying (15 liters/min) and nebulizing (3 liters/min) gas. The ion spray voltage was ±4,500 V. Data were acquired and analyzed using LabSolutions software, version 5.42SP4, from Shimadzu. Identification was achieved by comparison of experimental retention times and UV-MS spectra to bibliographic data and standard compounds.

Culture conditions. *Phanerochaete chrysosporium* homocaryon RP78 was maintained in malt agar medium. Fungal plugs were used to inoculate liquid minimal medium containing 5 mM sodium acetate, pH 4.5, 1% glucose, 1 mM ammonium tartrate, 1% (vol/vol) base medium (20 g liter^{-1} KH_2PO_4, 5 g liter^{-1} $MgSO_4$, 1 g liter^{-1} $CaCl_2$), 7% (vol/vol) trace medium [1.5 g liter^{-1} nitrilotriacetate, 3 g liter^{-1} $MgSO_4$, 1 g liter^{-1} NaCl, 0.1 g liter^{-1} $FeSO_4 \cdot 7H_2O$, 0.1 g liter^{-1} $CoCl_2$, 0.1 g liter^{-1} $ZnSO_4 \cdot 7H_2O$, 0.1 g liter^{-1} $CuSO_4$, 10 mg liter^{-1} $AlK(SO_4) \cdot 12H_2O$, 10 mg liter^{-1} H_3BO_3, 10 mg liter^{-1} $NaMoO_4 \cdot 2H_2O$], and 225 μM $MnCl_2$ (19). To study the effect of oak acetonic extracts on *P. chrysosporium* gene expression, static culturing was performed at 37°C for 3 days. The medium was then replaced by fresh liquid minimal medium (30 ml) as described above, with or without extracts obtained from 200 mg of oak wood. The treatment was done at 37°C for 24 h. The mycelium then was rinsed with distilled water and frozen in liquid nitrogen for further RNA extraction.

Arrays. The *P. chrysosporium* custom exon expression array (12×135K array) was manufactured by Roche NimbleGen Systems Ltd. (Madison, WI, USA). From a data set of 9,998 unique *P. chrysosporium* gene predictions, each array featured 6 unique probes per gene, all in duplicate.

Total RNA was extracted and purified from triplicate cultures using the RNeasy plant minikit (Qiagen) according to the manufacturer's instructions. The RNA was treated twice with DNase I (during purification as recommended in the manufacturer's protocol and directly added onto purified RNA) and cleaned with a Qiagen RNA cleanup kit. An additional purification step was performed to remove residual phenolic compounds due to oak treatment by precipitating RNA with 2 M LiCl. RNA was converted to double-stranded cDNA using the Smarter PCR cDNA synthesis kit (Clontech) according to the manufacturer's protocol and purified using the QIAquick PCR purification kit (Qiagen). Single-dye labeling of samples, hybridization procedures, data acquisition, background correction, and normalization were performed at the NimbleGen facilities (NimbleGen Systems, Reykjavik, Iceland) by following their standard protocol. Microarray probe intensities were quantile normalized across all chips. Average expression levels were calculated for each gene from the independent probes on the array and were used for further analysis. Natural log-transformed data were calculated and subjected to the Cyber-T statistical framework (http://cybert.ics.uci.edu/) (20) using the Standard *t* test unpaired two-conditions data module. Benjamini and Hochberg multiple-hypothesis testing corrections with false discovery rates (FDR) were used.

Transcripts with a significant *P* value (<0.05) were considered to be differentially expressed.

Cloning of PcGTT2.1 and heterologous expression and purification of the recombinant protein. The open reading frame sequence encoding *P. chrysosporium* GTT2.1 (PcGTT2.1; JGI ProtID 6766) was amplified from a *P. chrysosporium* cDNA library using PcGTT2.1 forward and reverse primers (5′ CCCCCATGGCTCACCTCCCCAACTTTCTC 3′ and 5′ CCCCGGATCCTTAGTGGAGGGTCTCGGC 3′) and cloned into the NcoI and BamHI restriction sites (underlined in the primers) of pET-3d (Novagen). The amplified sequences encoded a protein in which an alanine has been added to improve protein production. For protein production, the *Escherichia coli* BL21(DE3) strain, containing the pSBET plasmid, was cotransformed with PcGTT2.1-pET-3d plasmid (21). Cultures were progressively amplified up to 2 liters in LB medium supplemented with ampicillin and kanamycin at 37°C. Protein expression was induced at exponential phase by adding 100 μM isopropyl β-D-thiogalactopyranoside for 4 h at 37°C. The cultures then were centrifuged for 15 min at 4,400 × *g*. The pellets were resuspended in 30 ml of TE-NaCl (30 mM Tris-HCl, pH 8.0, 1 mM EDTA, 200 mM NaCl) buffer. Cell lysis was performed by sonication (3 times for 1 min each with intervals of 1 min), and the soluble and insoluble fractions were separated by centrifugation for 30 min at 27,000 × *g*. The soluble part then was fractionated with ammonium sulfate in two steps, and the protein fraction precipitating between 40 and 80% of the saturation contained the recombinant protein, as estimated by 15% SDS-PAGE. The protein was purified by size-exclusion chromatography after loading the resolubilized fraction on an ACA44 (5- by 75-cm) column equilibrated in TE-NaCl buffer. The fractions containing the protein were pooled, dialyzed by ultrafiltration to remove NaCl, and loaded onto a DEAE-cellulose column (Sigma) in TE (30 mM Tris-HCl [pH 8.0], 1 mM EDTA) buffer. The proteins were eluted using a 0 to 0.4 M NaCl gradient. Finally, the fractions of interest were pooled, dialyzed, concentrated by ultrafiltration under nitrogen pressure (YM10 membrane; Amicon), and stored in TE buffer at −20°C. Purity was checked by SDS-PAGE. Protein concentration was determined spectrophotometrically using a molar extinction coefficient at 280 nm of 60,390 M^{-1} cm^{-1}. A total of around 60 mg of pure PcGTT2.1 was obtained (final yield, 25 mg per liter of culture).

Activity measurements. The activity measurements of PcGTT2.1 in thiol transferase activity with hydroxyethyldisulfide (HED) assay or for reduction of dehydroascorbate (DHA) were performed at 25°C as described by Couturier and coworkers (22). The classical GSH transferase activity was assessed with phenethyl isothiocyanate (ITC) prepared in 2% (vol/vol) acetonitrile, 1-chloro-2,4-dinitrobenzene (CDNB) prepared in DMSO, and 4-hydroxynonenal (HNE) in ethanol as substrates (14, 23). The reactions were monitored at 274 nm for ITC, 340 nm for CDNB, and 224 nm for HNE following the increase in absorbance arising from the formation of the *S*-glutathionylated adduct. The reactions with CDNB were performed in 100 mM phosphate buffer, pH 7.5, in the presence of glutathione (2 mM), while the reaction with ITC was performed at pH 6.5

with an identical GSH concentration. The conjugation of HNE with GSH was monitored in 50 mM phosphate buffer, pH 6.5, at 30°C (23). The apparent K_{cat} value for HNE was determined in the presence of 2 mM GSH using an HNE range from 0 to 0.5 mM. Glutathione peroxidase activities were monitored as described previously (14): peroxide (hydrogen peroxide [H_2O_2], *tert*-butyl hydroperoxide [tBOOH], and cumene hydroperoxide [CuOOH]) in 30 mM Tris-HCl, pH 8.0, was incubated in the presence of GSH, 200 μM NADPH, and 0.5 IU glutathione reductase (GR). The activity was analyzed by monitoring the decrease in absorbance arising from NADPH oxidation in this coupled enzyme assay system showing the formation of oxidized glutathione (GSSG). The K_m value for GSH was determined using a GSH concentration ranging from 0 to 2 mM in the presence of 100 μM CuOOH. The apparent K_{cat} value for tBOOH was determined in the presence of 1 mM GSH using a tBOOH concentration ranging from 0 to 2 mM. The apparent K_{cat} value for CuOOH was determined in the presence of 1 mM GSH using a CuOOH range from 0 to 2 mM. The reactions were started by addition of the purified enzyme and monitored with a Cary 50 UV-visible spectrophotometer (Varian). The catalytic parameters were calculated using GraphPad software.

Yeast complementation. *Saccharomyces cerevisiae* strains W303-1A (*MAT***a** *ura3-1 ade2-1 leu2-3,112 trp1-1 his3-11,15 can1-1*) and MML1022 (W303-1A Δ*gtt1*::*natMX4* Δ*gtt2*::*kanMX4*) were employed. The MML1022 strain was constructed by standard genetic methods as described previously (24). MML1022 was transformed with either pCM190 or PcGTT2.1-pCM190 vector. The overexpression of PcGTT2.1 in the yeast strains was checked by Western blotting with rabbit polyclonal anti-PcGTT2.1 (1:1,000) using protein extracts (20 μg) from yeast cultures exponentially growing in SC supplemented with the required amino acids.

For sensitivity experiments, the growth of *S. cerevisiae* cells in liquid SD medium (25) under parallel separate treatments at 30°C was automatically recorded (by optical density at 600 nm) at 1-h intervals for 24 h, using individual 0.5-ml cultures in shaken microtiter plates sealed with oxygen-permeable plastic sheets, in a PowerWave XS (Biotek) apparatus at controlled temperature. Identical cell numbers (2×10^5) were inoculated initially in each parallel culture. Cells were treated with 0.2 mM tBOOH or 0.4 mM H_2O_2.

Lipid peroxidation measurement. Lipid peroxidation has been measured in *S. cerevisiae* mutant MML1022 and PcGTT2.1-complemented mutant strains in the presence of tBOOH. Cells (2×10^7) were grown in liquid SD medium for 2 h and then treated with 0.2 mM tBOOH for 4 h. The Bioxytech HAE-586 kit (OxisResearch) was used to measure 4-hydroxyalkenal (HAE), which is an indicator of lipid peroxidation. The protocol used is the one described by the manufacturer.

Microarray data accession number. The complete expression data set is available as a series (accession number GSE54542) at the Gene Expression Omnibus (GEO) at the National Center for Biotechnology Information (NCBI).

RESULTS AND DISCUSSION

Transcriptomic analysis. (i) Overview of gene expression. The effect of oak acetonic extracts on *P. chrysosporium* gene expression was assessed by transcriptome analysis. The complete transcriptomic data are given in Table S1 in the supplemental material. LC-MS analysis of these extracts revealed that they mainly contain caffeic acid, castalagin/vescalagin, and ellagic acid, which are tannin-derived molecules (see Table S2). Besides their antioxidant properties, these molecules have toxic and antimicrobial activities (26, 27). Indeed, tannins have the ability to bind strongly to proteins, often causing precipitation and inactivation of enzymes (28).

The most upregulated genes (more than 10-fold) by incubation with oak acetonic extracts are reported in Table 1. These genes encode proteins involved in nutrition, nucleic acid modification, gene regulation, signaling, and stress responses. A limited number of genes coding for proteins involved in degradation of recalcitrant compounds, respiration, and folate and methionine metabolism also were found among the most upregulated genes. The induction of genes involved in amino acid (lysine-ketoglutarate reductase, taurine dioxygenase, arginase, and fumarylacetoacetate hydralase) and protein (protease) catabolism could be a way to recycle both intracellular carbon and nitrogen. In accordance with this, the gene coding for glutamine synthetase also is induced. In addition, some genes involved in mitochondrial respiration are induced, suggesting modification of the bioenergetic state of the fungus.

Interestingly, the most upregulated gene encodes a protein (ProtID 2416) with an unknown function but with the characteristics of small secreted proteins (SSPs). Indeed, it is predicted to be secreted, the sequence is less than 300 amino acids, and it contains many cysteines. Such proteins have been studied recently in *Phlebia brevispora* and *Heterobasidion annosum* (29). The authors focused their analysis on hydrophobins. A considerable expansion of the hydrophobin-encoding genes exists in basidiomycetes, probably in relation to their ecological preferences. The gene identified in our analysis does not belong to the hydrophobin family, since it does not exhibit the conserved eight-cysteine motif and has not been identified as a hydrophobin in genomic analysis (30). SSPs are of great interest in pathology and symbiosis research, since they could act as signaling molecules in fungi and are able to regulate gene expression of the plant host (31, 32). A putative thaumatin-encoding gene also is induced. Although thaumatin genes are well studied in plants, they have been discovered only recently in fungi (33). In saprophytic fungi, the role of these proteins still is unknown, but a signaling function is plausible.

Stress-related genes could be noticed, such as the ones coding for a peptide methionine sulfoxide reductase or an acetyltransferase. The oxidation of methionine into methionine sulfoxide (MetSO) is a reversible process, the reduction being catalyzed by methionine sulfoxide reductase. These oxidation/reduction steps could restore the biological activity of proteins by repairing oxidative damage (34). Few GCN5-related N-acetyltransferases have been characterized in fungi. A study shows that MPR1, belonging to the GCN5-related N-acetyltransferase, is involved in stress responses in *S. cerevisiae*. Indeed, it has been shown to regulate ROS caused by a toxic proline catabolism intermediate (35).

An accumulation of flavonol reductase/cinnamoyl-coenzyme A (CoA) reductase transcripts also has been highlighted in the presence of oak acetonic extract. The corresponding enzyme is an oxidoreductase acting on cinnamaldehyde, an organic compound naturally occurring in the bark of the cinnamon tree. This enzyme participates in the lignin biosynthesis pathway (36). Moreover, a 9-fold-elevated level of cinnamoyl-CoA reductase protein in *P. chrysosporium* under Cu stress suggests a role of this enzyme in stress response (37). In addition to the genes reported in Table 1, 73 genes exhibiting no homology in the databases are upregulated more than 10-fold.

(ii) Extracellular degradation of lignocellulose and aromatic compounds. The induction of genes coding for enzymes involved in the extracellular degradation of aromatic compounds suggests putative extracellular oxidation of the tannin-derived molecules. Indeed, genes coding for a chloroperoxidase and a benzoquinone reductase and five genes coding for some class II peroxidases (lignin and manganese peroxidases) are induced by oak extracts

TABLE 1 Most upregulated genes (>10-fold) in the oak extract treatment compared to the control condition[a]

ProtID v2.0 and grouping	ProtID v2.2	Fold upregulation in oak vs control	Cyber-T		Annotation
			ppde,p	BH	
Degradation and nutrition					
40125	2919778	37.16	0.9996	4.95E−04	Aspartyl protease
9276	3043396	30.15	0.9984	1.96E−03	Lysine-ketoglutarate reductase/saccharopine dehydrogenase
130933	3043390	29.62	0.9981	2.49E−03	Lysine-ketoglutarate reductase/saccharopine dehydrogenase
34295	2889548	28.87	0.9779	3.30E−02	Chloroperoxidase
122114	3028920	24.75	0.9688	4.54E−02	Predicted transporter (major facilitator superfamily)
10661	2957918	21.67	0.9997	3.19E−04	Taurine catabolism dioxygenase, TauD/TfdA
4568	3033687	18.41	0.9905	1.41E−02	Arginase family protein
134181	3006107	16.28	0.9975	3.32E−03	Voltage-gated shaker-like K^+ channel, subunit beta/KCNAB/aryl-alcohol dehydrogenase
41330	2922705	15.64	0.9912	1.30E−02	Aromatic compound dioxygenase
5517	2911054	13.77	0.9942	8.39E−03	EXPN, distantly related to plant expansins
5864	2828877	13.73	0.9898	1.52E−02	Glutamine synthetase
137220	3015932	12.51	0.9886	1.71E−02	Predicted transporter (major facilitator superfamily)
9336	3021560	12.51	0.9946	7.73E−03	Predicted transporter (major facilitator superfamily)
132735	3001100	11.69	0.9702	4.38E−02	Predicted fumarylacetoacetate hydralase
37522	2972234	11.40	0.9978	2.87E−03	Glycoside hydrolase family 20 protein
137453	2966954	11.36	0.9999	8.73E−05	Glycosyltransferase family 2 protein
121193	121193	11.10	0.9882	1.76E−02	Lytic polysaccharide monooxygenase (formerly GH61)/carbohydrate-binding module family 1 protein
135277	2990792	10.79	0.9671	4.75E−02	Amino acid transporters
4296	2953754	10.62	0.9840	2.41E−02	Predicted transporter (major facilitator superfamily)
137216	3024803	10.42	0.9826	2.61E−02	Glycoside hydrolase family 7/carbohydrate-binding module family 1 protein
Folate/methionine pathway					
5290	2722858	11.86	0.9990	1.27E−03	Folylpolyglutamate synthase
123437	3034009	10.39	0.9991	1.10E−03	C_1-tetrahydrofolate synthase
125238	3032558	10.15	0.9996	4.44E−04	Methylthioadenosine phosphorylase (MTAP)
Respiration					
127904	2978093	17.30	0.9999	7.96E−05	Protein involved in ubiquinone biosynthesis
44349	2937022	16.81	0.9953	6.77E−03	NADH:ubiquinone oxidoreductase, NDUFS6, 13-kDa subunit
34038	2989470	13.99	0.9801	2.98E−02	Cytochrome *c* oxidase, subunit Va/COX6
6157	2957600	11.85	0.9986	1.71E−03	NADH-dehydrogenase (ubiquinone)
DNA/RNA modification, gene regulation					
5211	2983373	23.13	0.9999	1.18E−04	Nucleolar GTPase/ATPase p130
5606	5606	21.47	0.9875	1.86E−02	Splicing coactivator SRm160/300, subunit SRm300
8396	1637283	20.24	0.9977	3.01E−03	Splicing coactivator SRm160/300, subunit SRm300
6418	1283299	18.79	0.9938	9.06E−03	CCCH-type Zn-finger protein
2677	2677	18.20	0.9991	1.06E−03	Nucleolar GTPase/ATPase p130
130038	2976481	17.05	1.0000	2.38E−07	Inositol polyphosphate 5-phosphatase and related proteins
7242	2915258	13.78	0.9885	1.72E−02	Transcription factor of the Forkhead/HNF3 family
129920	2899842	12.44	0.9908	1.37E−02	Transcription factor TAFII-31
8180	2916937	10.95	0.9907	1.38E−02	Nuclear pore complex, rNup107 component (ScNup84)
5016	2668412	10.80	0.9753	3.70E−02	RNA polymerase II, large subunit
25553	2919747	10.64	0.9999	1.30E−04	Cullins
44155	2874226	10.42	0.9940	8.73E−03	Putative translation initiation inhibitor UK114/IBM1
139682	2898028	10.39	0.9976	3.24E−03	ATP-dependent RNA helicase
39851	2987670	10.31	0.9886	1.71E−02	Translational repressor MPT5/PUF4 and related RNA-binding proteins (Puf superfamily)
6343	2912954	10.24	0.9985	1.84E−03	Endoplasmic reticulum-to-Golgi-structure transport protein/RAD50-interacting protein 1
2869	2967072	10.20	0.9992	9.43E−04	Uncharacterized conserved protein/Zn-finger protein
32494	1905331	10.15	0.9989	1.40E−03	Nuclear localization sequence-binding protein
Signaling and stress					
2416	2901030	106.57	0.9993	8.71E−04	Unknown/SSP putative
41334	2904208	22.16	0.9992	9.71E−04	Flavonol reductase/cinnamoyl-CoA reductase

(Continued on following page)

TABLE 1 (Continued)

ProtID v2.0 and grouping	ProtID v2.2	Fold upregulation in oak vs control	Cyber-T ppde,p	Cyber-T BH	Annotation
5667	2984197	20.42	0.9979	2.75E−03	Tyrosine kinase specific for activated (GTP-bound) p21cdc42Hs
3280	3003339	18.81	0.9945	7.97E−03	Thaumatin
5747	3005309	17.85	0.9939	8.85E−03	Dual-specificity phosphatase
133796	2981209	15.18	0.9919	1.19E−02	Serine/threonine protein phosphatase
38902	2989411	14.09	0.9955	6.51E−03	Extracellular protein SEL-1 and related proteins
1088	2965634	13.41	0.9902	1.46E−02	RTA1-like protein
122315	122315	11.99	0.9989	1.42E−03	Peptide methionine sulfoxide reductase
43951	3032803	11.63	0.9985	1.95E−03	MAPEG
43149	2914358	11.28	0.9959	5.95E−03	GCN5-related *N*-acetyltransferase
136604	2907053	10.32	0.9913	1.29E−02	Thioredoxin/protein disulfide isomerase

[a] ProtID from *P. chrysosporium* v2.0 and v2.2 JGI databases are reported. Annotations are those retrieved from the v2.2 database. ppde,p, posterior probability of differential expression; BH, Benjamini and Hochberg. MAPEG, membrane-associated protein involved in eicosanoid and glutathione metabolism.

from 2.25- to 28.87-fold (Table 2). Consistent with the induction of these genes, other genes coding for enzymes that generate H_2O_2 (the copper radical oxidase cro1, pyranose oxidase, and oxalate oxidase) also are upregulated. However, while glyoxal oxidase has been suggested to be the predominant source of extracellular H_2O_2, no corresponding gene was upregulated under our conditions. Inversely, some other oxidases are downregulated by oak extracts (GMC oxidoreductase, copper radical oxidases cro4 and cro6, and oxalate oxidase). These results can be analyzed in light of a previous transcriptomic analysis of *P. chrysosporium* grown on oak wood (38). The cDNAs highly expressed in that study on wood material also are globally upregulated in our study. In particular, LipD (ProtID 6811) and MnP1 (ProtID 140708) have been identified in both studies, suggesting a putative signaling/regulatory role of phenolics for gene expression.

Genes coding for carbohydrate active enzymes (CAZymes) also have been found differentially expressed under our conditions (Table 3). Again, some of the genes induced by oak extracts are highly expressed in wood (38). This is the case for some cellobiohydrolases (ProtID 127029, 129072, and 133052), endoglucanases (ProtID 129325, 41563, and 31049), β-glucosidase (ProtID 8072), endoxylanase (ProtID 133788, 138715, and 138345), and acetyl xylan esterase (ProtID 130517) (Table 3; also see Table S1 in the supplemental material) (38). Inversely, we show a downregulation leading to very low expression of genes coding for alcohol oxidase (ProtID 126879), cellobiohydrolase (ProtID 137372), endoglucanase (ProtID 6458 and 8466), and endomannanase (ProtID 140501), while from 72 to 377 tags have been reported for these genes in the culture with oak. Since glucose was used as a carbon source in the present study, one can expect that in a natural biotope (glucose poor), more CAZY could be expressed. Indeed, it has been shown that cellulolytic and xylanolytic genes are regulated by transcriptional factors XYR1 and CRE1 in *Trichoderma reesei* depending on the carbon source, with glucose acting as a repressor (39).

(iii) Intracellular detoxification systems. Genes coding for proteins involved in the antioxidant response, such as methionine sulfoxide reductase and disulfide isomerase, are induced by oak acetonic extracts. Moreover, the induction of two glutathione reductase (GR1 and GR3) genes suggests an intracellular accumulation of oxidized glutathione, evidence for oxidative stress. However, another GR (GR2), which is predicted to be directed to

TABLE 2 Regulation of genes coding for the lignin degradation system[a]

ProtID v2.0	ProtID v2.2	Fold upregulation in oak vs control	Cyber-T ppde,p	Cyber-T BH	Annotation
34295	2889548	28.87	0.9779	3.30E−02	Chloroperoxidase
10307	2979875	7.16	1.0000	3.49E−05	Benzoquinone reductase BQR1
878	2896529	6.33	0.9727	4.08E−02	Class II peroxidase MnP
6811	1386770	4.26	0.9755	3.67E−02	Class II peroxidase LiPD
140708	8191	3.97	0.9661	4.87E−02	Class II peroxidase MnP1
6250	2911114	3.58	0.9834	2.49E−02	Class II peroxidase
124009	2416765	3.41	0.9829	2.57E−02	Copper radical oxidase cro1
131217	3003453	2.66	0.9854	2.19E−02	Oxalate oxidase/decarboxylase
137275	2977507	2.53	0.9661	4.87E−02	Pyranose oxidase pox
123914	123914	2.25	0.9909	1.36E−02	Class II peroxidase
129887	3008599	0.47	0.9814	2.80E−02	Benzoquinone reductase BQR3
6199	6199	0.20	0.9988	1.53E−03	GMC oxidoreductase
1932	3023991	0.16	0.9978	2.93E−03	Iron-binding glycoprotein
37905	2894758	0.12	0.9892	1.61E−02	Copper radical oxidase cro6
8882	1717398	0.10	0.9953	6.74E−03	Copper radical oxidase cro4
136169	2908112	0.06	0.9937	9.09E−03	Oxalate oxidase/decarboxylase

[a] Prot ID from *P. chrysosporium* v2.0 and v2.2 JGI databases are reported. Annotations are those retrieved from v2.2 and previous analyses (58, 63, 64).

TABLE 3 Regulation of genes coding for the CAZymes[a]

ProtID		Fold upregulation in oak vs control	Cyber-T		Annotation
v2.0	v2.2		ppde,p	BH	
37522	2972234	11.40	0.9978	2.87E−03	Glycoside hydrolase family 20
121193	2980158	11.10	0.9882	1.76E−02	Lytic polysaccharide monooxygenase (formerly GH61)
137216	3024803	10.42	0.9826	2.61E−02	Glycoside hydrolase family 7
40899	2978123	9.44	0.9905	1.41E−02	Glycoside hydrolase family 18
129072	2976248	8.97	0.9711	4.27E−02	Glycoside hydrolase family 7
42616	42616	7.56	0.9833	2.50E−02	Lytic polysaccharide monooxygenase (formerly GH61)
39389	2914306	5.14	1.0000	8.72E−06	Glycoside hydrolase family 16
4967	2982894	4.34	0.9791	3.12E−02	Lytic polysaccharide monooxygenase (formerly GH61)
1106	2965653	4.28	0.9654	4.95E−02	Six-hairpin glycosidase-like
9257	2919526	4.21	0.9758	3.63E−02	Glycoside hydrolase family 3
130517	2918304	4.09	0.9889	1.66E−02	Carbohydrate-binding module family 1/carbohydrate esterase family 15 protein
1924	2899497	3.27	0.9817	2.74E−02	Glycoside hydrolase family 85
138813	2909460	2.77	0.9980	2.64E−03	Glycoside hydrolase family 15/carbohydrate-binding module family 20
132605	2974311	2.75	0.9864	2.04E−02	Glycoside hydrolase family 63
121774	2989703	2.38	0.9821	2.69E−02	Glycoside hydrolase family 5
4590	2907097	2.12	0.9914	1.27E−02	Six-hairpin glycosidase-like
10320	3003776	0.04	0.9977	3.04E−03	Lytic polysaccharide monooxygenase (formerly GH61)
333	2896433	0.03	0.9999	8.05E−05	Glycoside hydrolase family 43
134001	3010808	0.03	1.0000	4.03E−06	Carbohydrate-binding module family 1/glycoside hydrolase family 27
140501	140501	0.03	1.0000	2.80E−05	Carbohydrate-binding module family 1/glycoside hydrolase family 5
4550	2579514	0.03	1.0000	4.85E−07	Glycoside hydrolase family 47
125033	3005667	0.02	0.9986	1.71E−03	Glycoside hydrolase family 27
128442	3003144	0.01	1.0000	1.83E−05	Glycoside hydrolase family 3

[a] Prot ID from *P. chrysosporium* v2.0 and v2.2 JGI databases are reported. Annotations are those retrieved from v2.2.

mitochondria, is downregulated. Similarly, a smaller amount of Mn-dependent superoxide dismutase transcripts has been detected under the oak extract conditions. This result is in accordance with oxidative stress at the mitochondrial level and with the induction of LiP expression by the intracellular ROS (3).

In accordance, YAP1, which is the central regulator of oxidative gene expression, is 5-fold induced. Moreover, the formation of peroxides inside the cell is supported by the upregulation of genes coding for a peroxiredoxin, PrxII.2, and a catalase. Focusing on the intracellular degradative pathways of toxic compounds, we highlighted the induction of 12 genes coding for CytP450 known as phase I detoxification enzymes and 5 and 3 genes coding for the phase II-conjugating glycosyl transferases (GT) and glutathione transferases, respectively (Table 4).

The CytP450ome has been quite extensively investigated in *P. chrysosporium*, especially thanks to a functional library in yeast (8, 9). These enzymes are highly versatile and inducible. The isoforms found induced in our experiment have not been functionally characterized yet, except for ProtID 7086 and 138612, which modify carbazole, dibenzothiophene, and ethoxycoumarin for the first one and naproxen for the second (9). Members from CYP5144 and CYP63 exhibit catalytic activities toward environmentally persistent and toxic high-molecular-weight polycyclic aromatic compounds, such as phenanthrene, pyrene or benzo(a)pyrene, alkylphenols, and alkane (40, 41). Evidence of the involvement of ProtID 131921 in the degradation of the endocrine disruptor chemical nonylphenol also has been demonstrated (42). Transcriptomic experiments showed that ProtID 139146 and 132579 gene expression is induced after anthracen and anthrone treatments (43). All of these studies demonstrate the potential of this enzyme family as biocatalysts to handle environmental mixed pollution. It is also important to note that many CytP450 genes are downregulated in our experiment.

The second detoxification phase consists of conjugating reactions performed by many transferases and, in particular, GTs and GSTs. GSTs are at the interface between compound elimination and oxidative stress rescue. In this study, we identified 3 GST genes, which are upregulated by oak acetonic extracts (MAPEG, GSTFuA3, and GTT2.1). The first gene encodes a membrane-associated protein involved in eicosanoid and glutathione metabolism (MAPEG). This superfamily includes structurally related membrane proteins with diverse functions of widespread origin. The eukaryotic MAPEG members can be subdivided into six families: MGST1, MGST2, and MGST3, leukotriene C-4 synthase (LTC4), 5-lipoxygenase activating protein (FLAP), and prostaglandin E synthase. Protein overexpression and enzyme activity analysis demonstrated that all proteins catalyzed the conjugation of CDNB with reduced glutathione. Thus, glutathione transferase activity can be regarded as a common denominator for a majority of MAPEG members throughout the kingdoms of life, whereas glutathione peroxidase activity occurs in representatives from the MGST1, MGST2, MGST3, and PGES subfamilies (44). Based on sequence homology, it appears that the *Phanerochaete* isoform belongs to MGST3, but it has not been functionally characterized yet. GSTFuA3 belongs to a newly identified GST class (18, 45). Four members of this class (GSTFuA1 to GSTFuA4) exhibit a

TABLE 4 Regulation of genes coding for the detoxification system[a]

ProtID v2.0 and grouping	ProtID v2.2	Fold upregulation in oak vs control	Cyber-T		Annotation
			ppde,p	BH	
Antioxidant system					
122315	122315	11.99	0.9989	1.42E−03	Methionine sulfoxide reductase MsrA
136604	2907053	10.32	0.9913	1.29E−02	Disulfide isomerase
135167	135167	8.54	0.9974	3.58E−03	Glutathione reductase GR3
7851	2915724	5.32	0.9817	2.75E−02	YAP1
125657	125657	4.08	0.9976	3.18E−03	Peroxiredoxin PrxII.2
128306	3025652	3.97	0.9902	1.46E−02	Catalase Cat1
876	2974699	2.29	0.9936	9.31E−03	Glutathione reductase GR1
127288	3002838	0.40	0.9863	2.07E−02	Catalase Cat3
127266	2013640	0.19	0.9915	1.26E−02	Catalase Cat5
10525	3027920	0.11	0.9999	7.06E−05	Glutathione reductase GR2
138910	2982879	0.01	1.0000	1.30E−08	Superoxide dismutase MnSOD2
Cytochrome P450 monooxygenases					
7086	3030400	8.21	0.9962	5.37E−03	CYP502B1
131322	2980309	7.24	0.9699	4.41E−02	CYP5144F1
131921	3029016	6.86	0.9742	3.87E−02	CYP5144C7
9146	2990306	5.81	0.9942	8.35E−03	
138612	2909718	5.80	0.9994	7.43E−04	CYP5035A2
137485	3081758	5.49	0.9994	7.11E−04	CYP63C2
38849	2974374	4.21	0.9958	6.09E−03	CYP5146A2
137321	2977643	3.99	0.9768	3.47E−02	CYP63C1
37971	2965345	2.64	0.9689	4.53E−02	CYP5144A11
139146	3035514	2.46	0.9954	6.63E−03	CYP5144C6
9478	2919941	2.32	0.9987	1.66E−03	CYP5140A1
132579	2897041	2.14	0.9901	1.48E−02	CYP5146B1
3368	2903228	0.04	0.9726	4.09E−02	CYP5141A2
1664	2976048	0.04	1.0000	2.56E−05	CYP5143A1
3661	3003571	0.04	0.9985	1.83E−03	CYP5147A2
38024	2895038	0.03	1.0000	1.45E−06	CYP5144A2
6327	3005638	0.03	1.0000	6.35E−06	CYP5145A3
798	2896486	0.02	1.0000	6.48E−06	CYP5144D5-CYP5144J1
8707	2989550	0.02	1.0000	9.28E−07	CYP512B2
8912	2963503	0.02	1.0000	3.03E−05	CYP5035B2
5055	2908523	0.01	1.0000	6.71E−06	CYP5144A12
38012	3090395	0.01	0.9999	5.22E−05	CYP5037A1
138753	2692082	0.01	1.0000	9.51E−07	CYP5144B1
761	3022655	0.01	1.0000	3.07E−06	CYP5144C2
5054	5054	0.01	0.9999	1.39E−04	CYP5144A13
Glycosyl transferases					
137453	2966954	11.36	0.9999	8.73E−05	GT family 2
3697	2904243	8.84	0.9814	2.79E−02	GT family 8
7550	1511835	8.07	0.9899	1.51E−02	GT family 8
2561	2901646	6.14	0.9769	3.46E−02	GT family 8
40855	2989061	5.08	0.9817	2.75E−02	GT family 3
1287	2898363	0.20	0.9999	1.33E−04	GT family 8
132866	3008474	0.06	0.9683	4.61E−02	GT family 4
125979	125979	0.02	1.0000	2.99E−05	GT family 8
Glutathione transferases					
43951	3032803	11.63	0.9985	1.95E−03	MAPEG
6766	3006031	8.51	0.9989	1.30E−03	GTT2.1
5122	2908587	5.07	0.9992	9.88E−04	GST FuA3
2268	2977134	0.05	0.9999	1.20E−04	Ure2p8
5118	2685965	0.33	0.9716	4.22E−02	GST FuA1
5119	2687275	0.12	0.9950	7.20E−03	GST FuA2

[a] Prot ID from *P. chrysosporium* v2.0 and v2.2 JGI databases are reported. Annotations are those retrieved from v2.2 and previous analyses (9, 63).

TABLE 5 Kinetic parameters of PcGTT2.1 in H_2O_2, tBOOH, CuOOH, and HNE activity assays compared to those of other fungal peroxidase-like enzymes[a]

Enzyme	Substrate								Reference or source
	H_2O_2		tBOOH		CuOOH		HNE		
	K_m (mM)	K_{cat} (s^{-1})	K_m (mM)	K_{cat} (s^{-1})	K_m (mM)	K_{cat} (s^{-1})	K_m (mM)	K_{cat} (s^{-1})	
PcGTT2.1	NA	NA	0.55 ± 0.24	725.00 ± 119.90	0.011 ± 0.002	500.00 ± 13.52	0.15 ± 0.03	0.78 ± 0.07	This study
ScGpx2	0.17	0.99	0.31	109.00	ND	ND	ND	ND	49
ScUre2p	4.30	0.36	7.90	0.07	7.80	0.37	ND	ND	50
PcGSTFuA3	NA	NA	NA	NA	2.04	1.27	ND	ND	14

[a] Experimental details are given in Materials and Methods. NA, not active; ND, not determined; Sc, *S. cerevisiae*; Pc, *P. chrysosporium*.

ligandin property toward wood compounds, such as coniferaldehyde, syringaldehyde, vanillin, chloronitrobenzoic acid, hydroxyacetophenone, and catechins, suggesting a role in sequestration and transport of the toxic molecules inside the cell (14, 45). GSTFuA3, which is the only member of this family that is able to reduce peroxides, is induced in our study, while GSTFuA1 and GSTFuA2 are downregulated. GTT2.1 was first defined by its sequence homology to GTT2 from *S. cerevisiae* (18). ScGTT2 exhibits GST activity with CDNB and seems to be crucial in the response to peroxides (46–48). However, no homologue has been characterized yet in other species. In *P. chrysosporium*, 2 genes have been identified: PcGTT2.1 (ProtID 6766) and PcGTT2.2 (ProtID 6683). While PcGTT2.1 is induced in our study (8.5-fold), PcGTT2.2 shows an expression ratio of only 1.8 in the oak extract treatment compared to the control (see Table S1 in the supplemental material).

Functional characterization of PcGTT2.1. (i) Enzymatic activities. The activity pattern of recombinant PcGTT2.1 has been determined using various substrates (Table 5). No thiol transferase and reductase activities with hydroxyethyl disulfide (HED) and dehydroascorbate (DHA) or GSH-transferase activity could be detected with the classical substrates CDNB and ITC. A weak GSH transferase activity has been measured with HNE, one of the major end products of lipid peroxidation. Moreover, PcGTT2.1 exhibited peroxidase activity with tBOOH and CuOOH but not with H_2O_2. With organic peroxides, the reaction catalyzed by PcGTT2.1 likely involves first a transfer of GSH onto the peroxide, which is rapidly removed by a second glutathione molecule to form GSSG and alcohol. This scheme was supported by the formation of GSSG that we have detected with NADPH-dependent GR method-based activity and mass spectrometry (data not shown). With peroxides as a substrate, the specific activity of PcGTT2.1 is substantially higher than that of fungal glutathione peroxidases. As an example, GPX2 from *S. cerevisiae* exhibits similar affinity but almost 7-fold-less activity than PcGTT2.1 toward tBOOH (49). Other fungal GSTs have been found to be able to reduce peroxides; however, they do so with less efficiency than PcGTT2.1 (14, 50) (Table 5). Moreover, PcGTT2.1 has a very strong affinity for CuOOH, suggesting high specificity for high-molecular-weight peroxides.

In humans, GST can modulate the intracellular concentrations of HNE by affecting its generation during lipid peroxidation by reducing hydroperoxides and also by converting it into a glutathione conjugate (51). Since PcGTT2.1 reacts with HNE, albeit rather slowly, it seems that it could be involved in both reactions. Thus, besides reducing oxidative stress, it could have a key role by

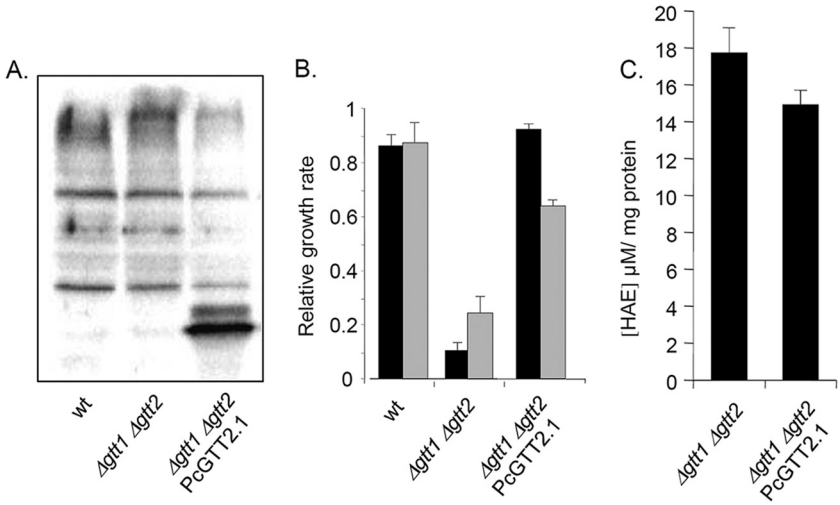

FIG 1 Functional analysis of PcGTT2.1. (A) Western blot confirming PcGTT2.1 overexpression in the yeast Δ*gtt1* Δ*gtt2* mutant. (B) Sensitivity of PcGTT2.1-complemented yeast strains to *tert*-butyl hydroperoxide (black bars) and hydrogen peroxide (gray bars). The growth of *S. cerevisiae* wild-type (wt; W303-1A) and Δ*gtt1* Δ*gtt2* mutant (MML1022) cells was automatically recorded as described in Materials and Methods. Exponential growth rates of treated cultures with the indicated agent concentrations, as well as control untreated cultures, were calculated, and the treated versus untreated ratios are represented. Bars correspond to the means from three independent experiments (plus standard deviations). (C) Measurement of 4-hydroxyalkenals (HAE) in Δ*gtt1* Δ*gtt2* mutants and in Δ*gtt1* Δ*gtt2* mutants complemented with PcGTT2.1. Bars correspond to the means from four independent experiments (plus standard deviations).

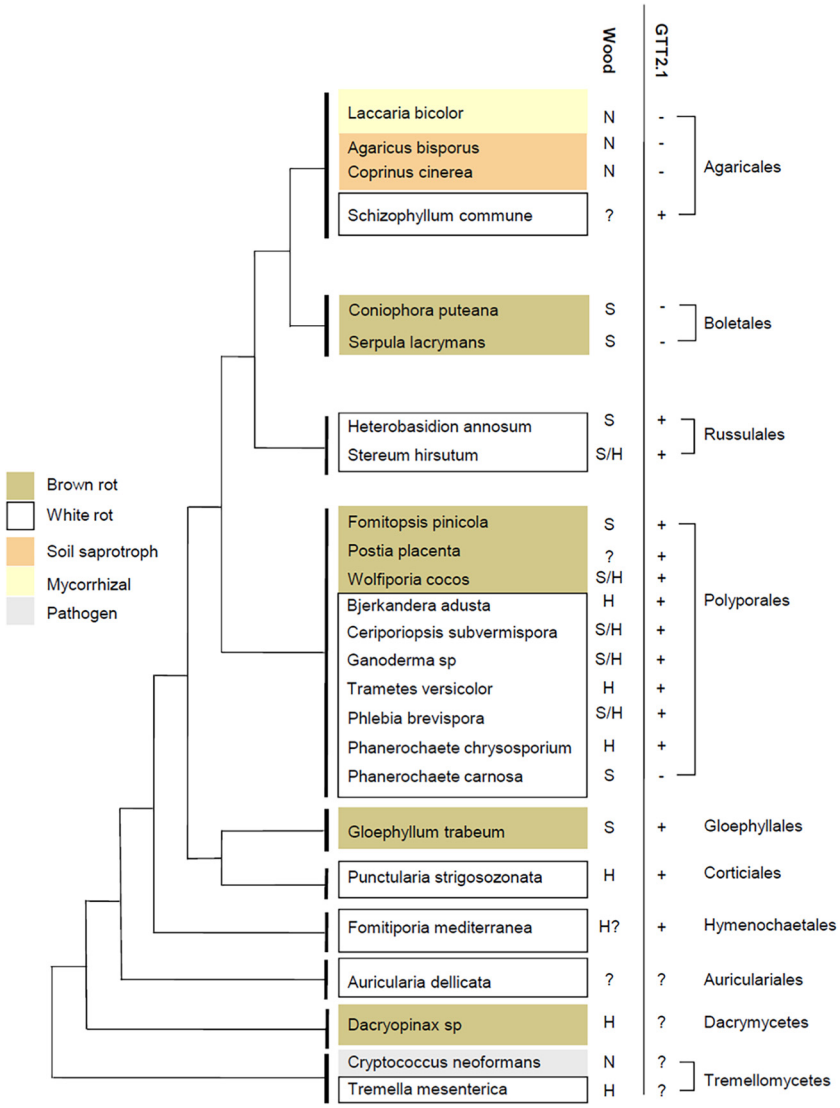

FIG 2 Presence of GTT2.1 gene in various basidiomycetes in relation to their taxonomic distribution and nutritional modes. Wood preference is reported. S, softwood; H, hardwood; N, nondegrader. This schematic tree has been constructed based on the chronogram made by Floudas et al. (58) and the phylogenetic tree shown in Fig. S1 in the supplemental material.

modulating HNE content, whose amount regulates stress signaling events and apoptosis.

(ii) Yeast complementation. PcGTT2.1 shares only 16.3% and 17.6% identity with ScGTT1 and ScGTT2, respectively, as defined by global sequence alignment using Lalign (http://www.ch.embnet.org/software/LALIGN_form.html). Nevertheless, the overexpression of PcGTT2.1 in a yeast strain deficient in both GTT1 and GTT2 genes rescued the growth of *S. cerevisiae* in the presence of H_2O_2 and tBOOH (Fig. 1A and B). While ScGTT2 displays only classical GSH transferase activity, ScGTT1 exhibits both classical GSH transferase activity and peroxidase activity with hydroperoxides (16). Moreover, it has been shown that exposure of GTT1/GTT2 double mutant strains to peroxides caused oxidative stress and increased lipid peroxidation (48). Lipid peroxides are unstable and decompose to form a complex series of malondialdehyde and HAE. HAE can be used as an indicator of lipid peroxidation (52). Under our conditions, less free 4-hydroxyalkenals were detected in the complemented strain compared to the mutant (Fig. 1C). This observation strengthens the proposal for a role of PcGTT2.1 in reducing lipid peroxidation *in vivo*.

(iii) Evolution of GTT2 genes. PcGTT2.1 orthologues have been searched in the available basidiomycete genomes from the MycoCosm database of the Joint Genome Institute (53). A phylogenetic analysis allowed us to identify 2 groups that we named GTT2.1 and GTT2.2 (see Fig. S1 in the supplemental material). In *P. chrysosporium*, both genes locate on the same scaffold; however, more than 200 kb separate them, suggesting that the duplication event is not very recent. While GTT2.2 orthologues have been identified in almost all other considered fungi except *Agaricus bisporus* and *Serpula lacrymans*, GTT2.1 gene losses could have occurred in the lineage leading to the *Boletales* and within lineages in the *Agaricales*, leading to the non-wood-decay species *Agaricus bisporus*, *Coprinopsis cinerea*, and *Laccaria bicolor* (Fig. 2). The presence of GTT2.1 was investigated in 15 mycorrhizal species

within the *Boletales* and *Agaricales* lineages, and only one orthologue was detected in *Suillus* species (data not shown). An interesting point is that *Phanerochaete carnosa*, which is a white rot fungus, does not exhibit any GTT2.1 homologue. While taxonomically close, *P. carnosa* and *P. chrysosporium* differ in that *P. carnosa* has been isolated almost exclusively from softwood, while *P. chrysosporium* was isolated mainly from hardwood. Globally, *P. carnosa* and *P. chrysosporium* similarly reduce the total phenolic content of various sapwood samples. *P. carnosa* transforms a higher fraction of phenolics in most of the heartwood samples, including those from softwood species, while *P. chrysosporium* transformed a broader range of heartwood phenolics in maple, a hardwood species (12). The accumulation of PcGTT2.1 transcripts in the presence of phenolics from oak heartwood suggests that PcGTT2.1 has a role in this process.

Looking at wood specificities of the various ligninolytic fungi, it is noticeable that all fungi growing on hardwood exhibit a GTT2.1 isoform. Softwood and hardwood fibers differ in the structure and composition of their hemicellulosic polymers and lignin (54). Indeed, softwood hemicelluloses are constituted mainly of galactoglucomannans and arabinoglucuronoxylans, while hardwood hemicelluloses contain mainly glucuronoxylans and glucomannans. Similarly, softwood lignins are mainly comprised of guaiacyl units, while hardwood lignins contain guaiacyl and syringyl units. The chemical composition of extractives depends directly on the wood species, and important variability exists among the ones mentioned above, leading to important variations in their content, chemical composition, and biological properties (55). A recent study showed that transgenic poplar lines enriched in syringyl lignin are more resistant to fungal degradation, suggesting a toxic effect of these subunits (56).

Given the detoxification activity of PcGTT2.1, our observation suggests a link between the maintenance of GTT2.1 in wood-degrader genomes and the selective pressure exerted by the toxic molecules released during wood degradation. It is an interesting point, since it suggests that the adaptation of fungi to their habitat occurs not only through their extracellular machinery of wood degradation (57, 58) but also through their ability to survive in toxic environments. A comparative genomic analysis did not reveal any differences in gene content for the classical antioxidant systems in *P. chrysosporium*, *C. cinereus*, and *L. bicolor* genomes (59). However, large variations have been observed in the detoxification system, including CytP450 and GSTs (11). These multigenic families obviously are good markers of adaptation.

Conclusions. Genomic, transcriptomic, and proteomic data have considerably enriched our knowledge concerning the regulation and evolution of wood degradation systems (12, 58, 60–62). Our transcriptomic analysis is original in that it focuses on the effect of oak-derived molecules, especially tannins, on *P. chrysosporium* gene expression. It reveals that in complement to the extracellular machinery of degradation, intracellular antioxidant and detoxification systems contribute to the lignolytic capabilities of fungi by preventing cellular damage and maintaining fungal health. In particular, the functional characterization of PcGTT2.1 suggests that the protein has evolved to specifically reduce lipid peroxidation during wood degradation. We believe that this is an interesting example of the neofunctionalization of a protein driven by selective pressure.

ACKNOWLEDGMENTS

The UMR IAM is supported by a grant overseen by the French National Research Agency (ANR) as part of the Investissements d'Avenir program (ANR-11-LABX-0002-01, Laboratory of Excellence ARBRE). This work also was supported by the French National Research Agency (project number ANR-09-BLAN-0012).

We have no conflicts of interest to declare.

REFERENCES

1. **Hunt CG, Houtman CJ, Jones DC, Kitin P, Korripally P, Hammel KE.** 2013. Spatial mapping of extracellular oxidant production by a white rot basidiomycete on wood reveals details of ligninolytic mechanism. Environ. Microbiol. **15:**956–966. http://dx.doi.org/10.1111/1462-2920.12039.
2. **Wei DS, Houtman CJ, Kapich AN, Hunt CG, Cullen D, Hammel KE.** 2010. Laccase and its role in production of extracellular reactive oxygen species during wood decay by the brown rot basidiomycete *Postia placenta*. Appl. Environ. Microbiol. **76:**2091–2097. http://dx.doi.org/10.1128/AEM.02929-09.
3. **Belinky PA, Flikshtein N, Lechenko S, Gepstein S, Dosoretz CG.** 2003. Reactive oxygen species and induction of lignin peroxidase in *Phanerochaete chrysosporium*. Appl. Environ. Microbiol. **69:**6500–6506. http://dx.doi.org/10.1128/AEM.69.11.6500-6506.2003.
4. **Feraydoni V, Hosseinihashemi SK.** 2012. Effect of walnut heartwood extractives, acid copper chromate, and boric acid on white-rot decay resistance of treated beech sapwood. Bioresources **7:**2393–2402.
5. **Ramirez MGL, Ruiz HGO, Arzate FN, Gallegos MAC, Enriquez SG.** 2012. Evaluation of fungi toxic activity of tannins and a tannin-copper complex from the mesocarp of *Cocos nucifera* Linn. Wood Fiber Sci. **44:**357–364.
6. **Wu CC, Wu CL, Huang SL, Chang HT.** 2012. Antifungal activity of liriodenine from *Michelia formosana* heartwood against wood-rotting fungi. Wood Sci. Technol. **46:**737–747. http://dx.doi.org/10.1007/s00226-011-0428-9.
7. **Dorado J, Claassen FW, van Beek TA, Lenon G, Wijnberg JB, Sierra-Alvarez R.** 2000. Elimination and detoxification of softwood extractives by white-rot fungi. J. Biotechnol. **80:**231–240. http://dx.doi.org/10.1016/S0168-1656(00)00264-9.
8. **Syed K, Yadav JS.** 2012. P450 monooxygenases (P450ome) of the model white rot fungus *Phanerochaete chrysosporium*. Crit. Rev. Microbiol. **38:**339–363. http://dx.doi.org/10.3109/1040841X.2012.682050.
9. **Hirosue S, Tazaki M, Hiratsuka N, Yanai S, Kabumoto H, Shinkyo R, Arisawa A, Sakaki T, Tsunekawa H, Johdo O, Ichinose H, Wariishi H.** 2011. Insight into functional diversity of cytochrome P450 in the white-rot basidiomycete *Phanerochaete chrysosporium*: involvement of versatile monooxygenase. Biochem. Biophys. Res. Commun. **407:**118–123. http://dx.doi.org/10.1016/j.bbrc.2011.02.121.
10. **Doddapaneni H, Chakraborty R, Yadav JS.** 2005. Genome-wide structural and evolutionary analysis of the P450 monooxygenase genes (P450ome) in the white rot fungus *Phanerochaete chrysosporium*: evidence for gene duplications and extensive gene clustering. BMC Genomics **6:**92. http://dx.doi.org/10.1186/1471-2164-6-92.
11. **Morel M, Meux E, Mathieu Y, Thuillier A, Chibani K, Harvengt L, Jacquot JP, Gelhaye E.** 2013. Xenomic networks variability and adaptation traits in wood decaying fungi. Microb. Biotechnol. **6:**248–263. http://dx.doi.org/10.1111/1751-7915.12015.
12. **Suzuki H, MacDonald J, Syed K, Salamov A, Hori C, Aerts A, Henrissat B, Wiebenga A, Vankuyk PA, Barry K, Lindquist E, LaButti K, Lapidus A, Lucas S, Coutinho P, Gong YC, Samejima M, Mahadevan R, Abou-Zaid M, de Vries RP, Igarashi K, Yadav JS, Grigoriev IV, Master ER.** 2012. Comparative genomics of the white-rot fungi, *Phanerochaete carnosa* and *P. chrysosporium*, to elucidate the genetic basis of the distinct wood types they colonize. BMC Genomics **13:**444. http://dx.doi.org/10.1186/1471-2164-13-444.
13. **Syed K, Shale K, Pagadala NS, Tuszynski J.** 2014. Systematic identification and evolutionary analysis of catalytically versatile cytochrome P450 monooxygenase families enriched in model basidiomycete fungi. PLoS One **9:**e86683. http://dx.doi.org/10.1371/journal.pone.0086683.
14. **Mathieu Y, Prosper P, Favier F, Harvengt L, Didierjean C, Jacquot JP, Morel-Rouhier M, Gelhaye E.** 2013. Diversification of fungal specific class A glutathione transferases in saprotrophic fungi. PLoS One **8:**e80298. http://dx.doi.org/10.1371/journal.pone.0080298.

15. **Collinson EJ, Grant CM.** 2003. Role of yeast glutaredoxins as glutathione S-transferases. J. Biol. Chem. **278:**22492–22497. http://dx.doi.org/10.1074/jbc.M301387200.
16. **Garcera A, Barreto L, Piedrafita L, Tamarit J, Herrero E.** 2006. *Saccharomyces cerevisiae* cells have three omega class glutathione S-transferases acting as 1-Cys thiol transferases. Biochem. J. **398:**187–196. http://dx.doi.org/10.1042/BJ20060034.
17. **Ma XX, Jiang YL, He YX, Bao R, Chen YX, Zhou CZ.** 2009. Structures of yeast glutathione-*S*-transferase GTT2 reveal a new catalytic type of GST family. EMBO Rep. **10:**1320–1326. http://dx.doi.org/10.1038/embor.2009.216.
18. **Morel M, Ngadin AA, Droux M, Jacquot JP, Gelhaye E.** 2009. The fungal glutathione S-transferase system. Evidence of new classes in the wood-degrading basidiomycete *Phanerochaete chrysosporium*. Cell. Mol. Life Sci. **66:**3711–3725. http://dx.doi.org/10.1007/s00018-009-0104-5.
19. **Tien M, Kirk TK.** 1988. Lignin peroxidase of *Phanerochaete chrysosporium*. Methods Enzymol. **161:**238–249. http://dx.doi.org/10.1016/0076-6879(88)61025-1.
20. **Baldi P, Long AD.** 2001. A Bayesian framework for the analysis of microarray expression data: regularized t-test and statistical inferences of gene changes. Bioinformatics **17:**509–519. http://dx.doi.org/10.1093/bioinformatics/17.6.509.
21. **Schenk PM, Baumann S, Mattes R, Steinbiss HH.** 1995. Improved high-level expression system for eukaryotic genes in *Escherichia coli* using T7 RNA polymerase and rare ArgtRNAs. Biotechniques **19:**196–200.
22. **Couturier J, Koh CS, Zaffagnini M, Winger AM, Gualberto JM, Corbier C, Decottignies P, Jacquot JP, Lemaire SD, Didierjean C, Rouhier N.** 2009. Structure-function relationship of the chloroplastic glutaredoxin S12 with an atypical WCSYS active site. J. Biol. Chem. **284:**9299–9310. http://dx.doi.org/10.1074/jbc.M807998200.
23. **Alin P, Danielson UH, Mannervik B.** 1985. 4-Hydroxyalk-2-enals are substrates for glutathione transferase. FEBS Lett. **179:**267–270. http://dx.doi.org/10.1016/0014-5793(85)80532-9.
24. **Barreto L, Garcera A, Jansson K, Sunnerhagen P, Herrero E.** 2006. A peroxisomal glutathione transferase of *Saccharomyces cerevisiae* is functionally related to sulfur amino acid metabolism. Eukaryot. Cell **5:**1748–1759. http://dx.doi.org/10.1128/EC.00216-06.
25. **Sherman F.** 2002. Getting started with yeast. Methods Enzymol. **350:**3–41. http://dx.doi.org/10.1016/S0076-6879(02)50954-X.
26. **Stojkovic D, Petrovic J, Sokovic M, Glamoclija J, Kukic-Markovic J, Petrovic S.** 2013. *In situ* antioxidant and antimicrobial activities of naturally occurring caffeic acid, p-coumaric acid and rutin, using food systems. J. Sci. Food Agric. **93:**3205–3208. http://dx.doi.org/10.1002/jsfa.6156.
27. **Field FA, Lettinga J.** 1992. Toxicity of tannic compounds to microorganisms, p 673–692. *In* Hemingway RW, Laks PE (ed), Plant polyphenols: synthesis, properties, significance. Basic life sciences, vol. 59. Plenum Press, New York, NY.
28. **Bennick A.** 2002. Interaction of plant polyphenols with salivary proteins. Crit. Rev. Oral Biol. Med. **13:**184–196. http://dx.doi.org/10.1177/154411130201300208.
29. **Mgbeahuruike AC, Kovalchuk A, Chen H, Ubhayasekera W, Asiegbu FO.** 2013. Evolutionary analysis of hydrophobin gene family in two wood-degrading basidiomycetes, *Phlebia brevispora* and *Heterobasidion annosum* s.l. BMC Evol. Biol. **13:**240. http://dx.doi.org/10.1186/1471-2148-13-240.
30. **Mgbeahuruike AC, Kovalchuk A, Asiegbu FO.** 2013. Comparative genomics and evolutionary analysis of hydrophobins from three species of wood-degrading fungi. Mycologia **105:**1471–1478. http://dx.doi.org/10.3852/13-077.
31. **Hacquard S, Joly DL, Lin YC, Tisserant E, Feau N, Delaruelle C, Legue V, Kohler A, Tanguay P, Petre B, Frey P, Van de Peer Y, Rouze P, Martin F, Hamelin RC, Duplessis S.** 2012. A comprehensive analysis of genes encoding small secreted proteins identifies candidate effectors in *Melampsora larici-populina* (poplar leaf rust). Mol. Plant Microbe Interact. **25:**279–293. http://dx.doi.org/10.1094/MPMI-09-11-0238.
32. **Plett JM, Kemppainen M, Kale SD, Kohler A, Legue V, Brun A, Tyler BM, Pardo AG, Martin F.** 2011. A secreted effector protein of *Laccaria bicolor* is required for symbiosis development. Curr. Biol. **21:**1197–1203. http://dx.doi.org/10.1016/j.cub.2011.05.033.
33. **Petre B, Major I, Rouhier N, Duplessis S.** 2011. Genome-wide analysis of eukaryote thaumatin-like proteins (TLPs) with an emphasis on poplar. BMC Plant Biol. **11:**33. http://dx.doi.org/10.1186/1471-2229-11-33.
34. **Levine RL, Mosoni L, Berlett BS, Stadtman ER.** 1996. Methionine residues as endogenous antioxidants in proteins. Proc. Natl. Acad. Sci. U. S. A. **93:**15036–15040. http://dx.doi.org/10.1073/pnas.93.26.15036.
35. **Nomura M, Takagi H.** 2004. Role of the yeast acetyltransferase MPR1 in oxidative stress: regulation of oxygen reactive species caused by a toxic proline catabolism intermediate. Proc. Natl. Acad. Sci. U. S. A. **101:**12616–12621. http://dx.doi.org/10.1073/pnas.0403349101.
36. **Li L, Cheng X, Lu S, Nakatsubo T, Umezawa T, Chiang VL.** 2005. Clarification of cinnamoyl co-enzyme A reductase catalysis in monolignol biosynthesis of aspen. Plant Cell Physiol. **46:**1073–1082. http://dx.doi.org/10.1093/pcp/pci120.
37. **Ozcan S, Yildirim V, Kaya L, Albrecht D, Becher D, Hecker M, Ozcengiz G.** 2007. *Phanerochaete chrysosporium* soluble proteome as a prelude for the analysis of heavy metal stress response. Proteomics **7:**1249–1260. http://dx.doi.org/10.1002/pmic.200600526.
38. **Sato S, Feltus FA, Iyer P, Tien M.** 2009. The first genome-level transcriptome of the wood-degrading fungus *Phanerochaete chrysosporium* grown on red oak. Curr. Genet. **55:**273–286. http://dx.doi.org/10.1007/s00294-009-0243-0.
39. **Castro LDS, Antoniêto AC, Pedersoli WR, Silva-Rocha R, Persinoti GF, Silva RN.** 2014. Expression pattern of cellulolytic and xylanolytic genes regulated by transcriptional factors XYR1 and CRE1 are affected by carbon source in Trichoderma reesei. Gene Expr. Patterns **14:**88–95. http://dx.doi.org/10.1016/j.gep.2014.01.003.
40. **Syed K, Doddapaneni H, Subramanian V, Lam YW, Yadav JS.** 2010. Genome-to-function characterization of novel fungal P450 monooxygenases oxidizing polycyclic aromatic hydrocarbons (PAHs). Biochem. Biophys. Res. Commun. **399:**492–497. http://dx.doi.org/10.1016/j.bbrc.2010.07.094.
41. **Syed K, Porollo A, Lam YW, Grimmett PE, Yadav JS.** 2013. Cyp63a2, a catalytically versatile fungal P450 monooxygenase capable of oxidizing higher-molecular-weight polycyclic aromatic hydrocarbons, alkylphenols, and alkanes. Appl. Environ. Microbiol. **79:**2692–2702. http://dx.doi.org/10.1128/AEM.03767-12.
42. **Subramanian V, Yadav JS.** 2009. Role of P450 monooxygenases in the degradation of the endocrine-disrupting chemical nonylphenol by the white rot fungus *Phanerochaete chrysosporium*. Appl. Environ. Microbiol. **75:**5570–5580. http://dx.doi.org/10.1128/AEM.02942-08.
43. **Chigu NL, Hirosue S, Nakamura C, Teramoto H, Ichinose H, Wariishi H.** 2010. Cytochrome P450 monooxygenases involved in anthracene metabolism by the white-rot basidiomycete *Phanerochaete chrysosporium*. Appl. Microbiol. Biotechnol. **87:**1907–1916. http://dx.doi.org/10.1007/s00253-010-2616-1.
44. **Bresell A, Weinander R, Lundqvist G, Raza H, Shimoji M, Sun TH, Balk L, Wiklund R, Eriksson J, Jansson C, Persson B, Jakobsson PJ, Morgenstern R.** 2005. Bioinformatic and enzymatic characterization of the MAPEG superfamily. FEBS J. **272:**1688–1703. http://dx.doi.org/10.1111/j.1742-4658.2005.04596.x.
45. **Mathieu Y, Prosper P, Buee M, Dumarcay S, Favier F, Gelhaye E, Gerardin P, Harvengt L, Jacquot JP, Lamant T, Meux E, Mathiot S, Didierjean C, Morel M.** 2012. Characterization of a *Phanerochaete chrysosporium* glutathione transferase reveals a novel structural and functional class with ligandin properties. J. Biol. Chem. **287:**39001–39011. http://dx.doi.org/10.1074/jbc.M112.402776.
46. **Choi JH, Lou W, Vancura A.** 1998. A novel membrane-bound glutathione S-transferase functions in the stationary phase of the yeast *Saccharomyces cerevisiae*. J. Biol. Chem. **273:**29915–29922. http://dx.doi.org/10.1074/jbc.273.45.29915.
47. **Herrero E, Ros J, Tamarit J, Belli G.** 2006. Glutaredoxins in fungi. Photosynth. Res. **89:**127–140. http://dx.doi.org/10.1007/s11120-006-9079-3.
48. **Mariani D, Mathias CJ, da Silva CG, Herdeiro RD, Pereira R, Panek AD, Eleutherio ECA, Pereira MD.** 2008. Involvement of glutathione transferases, Gtt1 and Gtt2, with oxidative stress response generated by H_2O_2 during growth of *Saccharomyces cerevisiae*. Redox Rep. **13:**246–254. http://dx.doi.org/10.1179/135100008X309028.
49. **Tanaka T, Izawa S, Inoue Y.** 2005. Gpx2, encoding a phospholipid hydroperoxide glutathione peroxidase homologue, codes for an atypical 2-Cys peroxiredoxin in *Saccharomyces cerevisiae*. J. Biol. Chem. **280:**42078–42087. http://dx.doi.org/10.1074/jbc.M508622200.
50. **Bai M, Zhou JM, Perrett S.** 2004. The yeast prion protein Ure2 shows glutathione peroxidase activity in both native and fibrillar forms. J. Biol. Chem. **279:**50025–50030. http://dx.doi.org/10.1074/jbc.M406612200.
51. **Awasthi YC, Yang Y, Tiwari NK, Patrick B, Sharma A, Li J, Awasthi S.** 2004. Regulation of 4-hydroxynonenal-mediated signaling by glutathione

S-transferases. Free Radic. Biol. Med. **37:**607–619. http://dx.doi.org/10.1016/j.freeradbiomed.2004.05.033.

52. **Esterbauer H, Schaur RJ, Zollner H.** 1991. Chemistry and biochemistry of 4-hydroxynonenal, malonaldehyde and related aldehydes. Free Radic. Biol. Med. **11:**81–128. http://dx.doi.org/10.1016/0891-5849(91)90192-6.
53. **Grigoriev IV, Nordberg H, Shabalov I, Aerts A, Cantor M, Goodstein D, Kuo A, Minovitsky S, Nikitin R, Ohm RA, Otillar R, Poliakov A, Ratnere I, Riley R, Smirnova T, Rokhsar D, Dubchak I.** 2012. The genome portal of the Department of Energy Joint Genome Institute. Nucleic Acids Res. **40:**D26–D32. http://dx.doi.org/10.1093/nar/gkr947.
54. **Sjöström E.** 1981. Wood polysaccharides, p 49–82. Wood chemistry: fundamentals and applications. Academic Press, New York, NY.
55. **Fengel D, Wegener G.** 1984. Chemical composition and analysis of wood, p 183–267. *In* de Gruyter W (ed), Wood chemistry, ultrastructures, reactions. Remagen, Berlin, Germany.
56. **Skyba O, Douglas CJ, Mansfield SD.** 2013. Syringyl-rich lignin renders poplars more resistant to degradation by wood decay fungi. Appl. Environ. Microbiol. **79:**2560–2571. http://dx.doi.org/10.1128/AEM.03182-12.
57. **Eastwood DC, Floudas D, Binder M, Majcherczyk A, Schneider P, Aerts A, Asiegbu FO, Baker SE, Barry K, Bendiksby M, Blumentritt M, Coutinho PM, Cullen D, de Vries RP, Gathman A, Goodell B, Henrissat B, Ihrmark K, Kauserud H, Kohler A, LaButti K, Lapidus A, Lavin JL, Lee YH, Lindquist E, Lilly W, Lucas S, Morin E, Murat C, Oguiza JA, Park J, Pisabarro AG, Riley R, Rosling A, Salamov A, Schmidt O, Schmutz J, Skrede I, Stenlid J, Wiebenga A, Xie XF, Kues U, Hibbett DS, Hoffmeister D, Hogberg N, Martin F, Grigoriev IV, Watkinson SC.** 2011. The plant cell wall-decomposing machinery underlies the functional diversity of forest fungi. Science **333:**762–765. http://dx.doi.org/10.1126/science.1205411.
58. **Floudas D, Binder M, Riley R, Barry K, Blanchette RA, Henrissat B, Martinez AT, Otillar R, Spatafora JW, Yadav JS, Aerts A, Benoit I, Boyd A, Carlson A, Copeland A, Coutinho PM, de Vries RP, Ferreira P, Findley K, Foster B, Gaskell J, Glotzer D, Gorecki P, Heitman J, Hesse C, Hori C, Igarashi K, Jurgens JA, Kallen N, Kersten P, Kohler A, Kues U, Kumar TKA, Kuo A, LaButti K, Larrondo LF, Lindquist E, Ling A, Lombard V, Lucas S, Lundell T, Martin R, McLaughlin DJ, Morgenstern I, Morin E, Murat C, Nagy LG, Nolan M, Ohm RA, Patyshakuliyeva A, Rokas A, Ruiz-Duenas FJ, Sabat G, Salamov A, Samejima M, Schmutz J, Slot JC, John FS, Stenlid J, Sun H, Sun S, Syed K, Tsang A, Wiebenga A, Young D, Pisabarro A, Eastwood DC, Martin F, Cullen D, Grigoriev IV, Hibbett DS.** 2012. The paleozoic origin of enzymatic lignin decomposition reconstructed from 31 fungal genomes. Science **336:**1715–1719. http://dx.doi.org/10.1126/science.1221748.
59. **Morel M, Kohler A, Martin F, Gelhaye E, Rouhier N.** 2008. Comparison of the thiol-dependent antioxidant systems in the ectomycorrhizal *Laccaria bicolor* and the saprotrophic *Phanerochaete chrysosporium*. New Phytol. **180:**391–407. http://dx.doi.org/10.1111/j.1469-8137.2008.02498.x.
60. **Fernandez-Fueyo E, Ruiz-Duenas FJ, Ferreira P, Floudas D, Hibbett DS, Canessa P, Larrondo LF, James TY, Seelenfreund D, Lobos S, Polanco R, Tello M, Honda Y, Watanabe T, San RJ, Kubicek CP, Schmoll M, Gaskell J, Hammel KE, St. John FJ, Vanden Wymelenberg A, Sabat G, BonDurant SS, Syed K, Yadav JS, Doddapaneni H, Subramanian V, Lavin JL, Oguiza JA, Perez G, Pisabarro AG, Ramirez L, Santoyo F, Master E, Coutinho PM, Henrissat B, Lombard V, Magnuson JK, Kues U, Hori C, Igarashi K, Samejima M, Held BW, Barry KW, LaButti KM, Lapidus A, Lindquist EA, Lucas SM, Riley R, Salamov AA, Hoffmeister D, Schwenk D, Hadar Y, Yarden O, de Vries RP, Wiebenga A, Stenlid J, Eastwood D, Grigoriev IV, Berka RM, Blanchette RA, Kersten P, Martinez AT, Vicuna R, Cullen D.** 2012. Comparative genomics of *Ceriporiopsis subvermispora* and *Phanerochaete chrysosporium* provide insight into selective ligninolysis. Proc. Natl. Acad. Sci. U. S. A. **109:**5458–5463. http://dx.doi.org/10.1073/pnas.1119912109.
61. **Kang YM, Prewitt ML, Diehl SV.** 2009. Proteomics for biodeterioration of wood (*Pinus taeda* L.): challenging analysis by 2-D PAGE and MALDI-TOF/TOF/MS. Int. Biodeterior. Biodegrad. **63:**1036–1044. http://dx.doi.org/10.1016/j.ibiod.2009.07.008.
62. **MacDonald J, Suzuki H, Master ER.** 2012. Expression and regulation of genes encoding lignocellulose-degrading activity in the genus Phanerochaete. Appl. Microbiol. Biotechnol. **94:**339–351. http://dx.doi.org/10.1007/s00253-012-3937-z.
63. **Morel M, Ngadin AA, Jacquot JP, Gelhaye E.** 2009. Reactive oxygen species in *Phanerochaete chrysosporium*. Relationship between extracellular oxidative and intracellular antioxidant systems. Adv. Bot. Res. **52:**153–186. http://dx.doi.org/10.1016/S0065-2296(10)52006-8.
64. **Vanden Wymelenberg A, Gaskell J, Mozuch M, Kersten P, Sabat G, Martinez D, Cullen D.** 2009. Transcriptome and secretome analyses of *Phanerochaete chrysosporium* reveal complex patterns of gene expression. Appl. Environ. Microbiol. **75:**4058–4068. http://dx.doi.org/10.1128/AEM.00314-09.